Electronic Supplementary Information

Electronic and Photophysical Properties of $Re^{I}(CO)_3Br$ Complexes Modulated by Pyrazolyl-Pyridazine Ligands

by the authors

Marianela Saldías,[⊥a] Nicolás Guzmán,[a] Franco Palominos,[a] Catalina Sandoval-Altamirano,[a] Germán Günther,[b] Nancy Pizarro,[a] Andrés Vega*[a,c]

[a] Universidad Andrés Bello, Departamento de Ciencias Químicas, Facultad de Ciencias Exactas, Av. Quillota 980, Viña del Mar, Chile.
[b] Universidad de Chile, Departamento de Química Orgánica y Fisicoquímica, Facultad de Ciencias Químicas y Farmacéuticas, Sergio Livingstone 1007, Santiago, Chile.
[c] Centro para el Desarrollo de la Nanociencia y la Nanotecnología, CEDENNA

[*] *Contact Author:* andresvega@unab.cl

[⊥]: Current Address: Instituto de Investigación e Innovación en Salud, Facultad de Ciencias de la Salud, Universidad Central, Lord Cochrane 417, Santiago, Chile

Table S1. Crystal data and structure refinement details for **I** to **V** (Solvent is not reported for **IV** and **V**).

	I	**II**	**III**	**IV**	**IV**
Formula	$C_{10}H_6N_4O_3BrRe$	$C_{10}H_5N_4O_3BrClRe$	$C_{13}H_{10}N_4O_5BrRe$	$C_{13}H_8N_6O_3BrRe$	$C_{15}H_{12}N_6O_3BrRe$
FW/uma	496.30	530.74	568.36	562.35	590.40
Crystal System	Monoclinic	Monoclinic	Monoclinic	Monoclinic	Triclinic
Space Group	$P2_1/n$	P21/c	$P2_1/c$	C2/c	$P\bar{1}$
a (Å)	8.2338(10)	7.0174(17)	8.1241(2)	24.814(11)	8.2045(14)
b (Å)	17.933(2)	16.124(4)	16.6942(5)	7.511(3)	10.8942(19)
c (Å)	9.1398(11)	12.405(3)	12.3835(5)	22.011(10)	11.726(2)
α (°)	90	90	90	90	91.137(2)
β (°)	96.823(2)	101.957(3)	107.837(3)	92.314(5)	91.184(2)
γ (°)	90	90	90	90	102.083(2)
V (Å^3)	1340.0(3)	1373.2 (6)	1598.78(9)	4099(3)	1024.3(3)
Z	4(4)	4(4)	4(4)	8(8)	2(2)
d (g cm^{-3})	2.460	2.567	2.361	1.823	1.915
μ (mm^{-1})	12.03	11.96	10.13	7.91	7.91
F000	912	976	1064	2360	556
θ range	2.3 to 26.0°	2.1 to 26.0°	2.3 to 26.0°	2.8 to 26.0°	1.7 to 26.0°
hkl range	$-10 \le h \le 10$	$-8 \le h \le 8$	$-10 \le h \le 10$	$-30 \le h \le 30$	$-10 \le h \le 10$
	$-22 \le k \le 22$	$-19 \le k \le 19$	$-20 \le k \le 20$	$-9 \le k \le 9$	$-13 \le k \le 13$
	$-11 \le l \le 11$	$-15 \le l \le 15$	$-15 \le l \le 14$	$-27 \le l \le 27$	$-14 \le l \le 14$
N_{tot}, N_{uniq} (R_{int}), N_{obs}	7570, 2614(0.040), 2020	9865, 2695(0.034), 2391	10633, 3129(0.078), 2298	14469, 3972(0.224), 2382	8025, 4018(0.036), 3591
Refinement Parameters	173	182	220	217	237
GOF	1.02	1.04	1.03	1.01	1.01
R1, wR2 (obs)	0.033, 0.075	0.024, 0.054	0.044, 0.095	0.084, 0.240	0.020, 0.045
Max. and min Δρ	1.46 and -0.87	2.35, -0.73	1.56 and -1.03	2.62 and –1.59	0.65 and -0.74

Table S2. Selected bond distances (Å), angles (°) and torsion angles (°) for compounds **I**-**V** as determined by X-rays diffraction compared to those computed from optimized models (DFT, Gas Phase).

	I		**II**		**III**		**IV**		**V**	
	RX	**DFT**	**RX**	**DFT**	**RX**	**DFT**	**RX**	**DFT**	**RX**	**DFT**
Re1—C13	1.908(8)	1.935	1.933(5)	1.936	1.918(10)	1.936	1.96(3)	1.931	1.927 (4)	1.930
Re1—C14	1.918(8)	1.933	1.912(5)	1.934	1.919(10)	1.932	1.99(2)	1.934	1.916 (4)	1.932
Re1—C15	1.929(9)	1.919	1.922(5)	1.920	1.898(11)	1.918	1.95(2)	1.920	1.915 (4)	1.918
Re1—N1	2.164(6)	2.189	2.154(4)	2.187	2.153(7)	2.193	2.146(13)	2.191	2.171 (3)	2.205
Re1—N3	2.170(5)	2.192	2.162(4)	2.189	2.138(7)	2.181	2.148(12)	2.192	2.175 (3)	2.193
Re1—Br1	2.6240(9)	2.668	2.6402(8)	2.666	2.6493(12)	2.671	2.633(2)	2.665	2.6219 (4)	2.666
C13—Re1—C14	88.4(3)	90.3	91.2(2)	90.3	88.9(4)	88.9	86.6(8)	90.5	89.72(16)	89.5
C13—Re1—C15	90.6(3)	90.9	90.7(2)	90.3	89.9(4)	90.8	90.1(8)	90.9	89.31(15)	90.9
C14—Re1—C15	91.2(3)	91.2	88.4(2)	91.2	91.2(5)	91.3	91.7(7)	91.2	89.03(16)	91.3
C13—Re1—N1	171.7(3)	169.4	169.4(2)	169.7	169.4(3)	168.5	101.6(7)	169.3	169.55(12)	168.5
C14—Re1—N1	99.1(3)	98.4	96.8(2)	98.2	101.7(3)	100.9	170.6(7)	98.6	99.91(14)	100.5
C15—Re1—N1	92.8(3)	98.4	96.4(2)	94.9	90.9(4)	94.9	92.9(6)	94.4	94.87(12)	94.5
C13—Re1—N3	98.1(3)	97.2	98.2(2)	97.4	96.1(3)	96.6	173.7(6)	96.9	96.31(13)	95.9
C14—Re1—N3	172.6(3)	170.4	170.5(2)	170.1	172.6(4)	171.5	97.8(7)	170.4	172.96(13)	172.0
C15—Re1—N3	92.3(3)	94.8	92.4(2)	94.8	94.4(4)	95.0	94.4(6)	95.0	94.67(12)	94.4
N1—Re1—N3	74.2(2)	73.5	73.7(1)	73.5	73.3(3)	73.0	73.6(5)	73.5	73.83(10)	73.5
C13—Re1—Br1	91.6(2)	91.3	87.7(2)	91.3	92.9(3)	91.7	92.7(5)	91.3	91.84(11)	91.7
C14—Re1—Br1	92.8(2)	91.2	93.1(1)	91.1	90.2(3)	90.3	90.2(5)	91.2	91.69(12)	91.0
C15—Re1—Br1	175.5(2)	176.8	177.9(1)	176.9	176.8(3)	176.7	176.7(6)	176.7	178.65(10)	176.6
N1—Re1—Br1	84.6(2)	82.6	84.9(1)	82.7	86.1(2)	82.3	84.8(3)	83.0	83.88(7)	82.6
N3—Re1—Br1	83.5(2)	82.6	86.3(1)	82.6	84.0(2)	82.5	82.8(3)	82.5	84.50(7)	83.1
N1—N2—C4—N3	-5.2(9)	-1.0	-8.6(6)	1.2	-4.3(12)	0.6	1.9(2)	1.4	-3.6(4)	-1.0
N4—C7—C16—O1					-3.6(15)	1.3				
N4—C7—N5—N6							0.3(2)	3.8	-172.7(3)	-176.7

Table S3. Summary of main energy, wavelength and oscillator strength computed for observed transitions in the absorption spectra of $\mathbf{L_I}$ – $\mathbf{L_V}$ and **I** – **V**, together with the orbitals implied.

N	E / eV	λ / nm	*f*	Major Contributions
				I
2	2.16	574	0.023	HOMO-1 → LUMO (97 %)
8	3.30	376	0.078	HOMO-4 → LUMO (80 %)
				HOMO-3 → LUMO+1 (12 %)
9	3.43	361	0.049	HOMO-4 → LUMO (12 %)
				HOMO-3 → LUMO+1 (85 %)
10	3.52	352	0.011	HOMO-4 → LUMO+1 (96 %)
12	3.98	312	0.013	HOMO-5 → LUMO+1 (11 %)
				HOMO → LUMO+2 (68 %)
				HOMO → LUMO+5 (10 %)
15	4.14	300	0.012	HOMO-1 → LUMO+4 (20 %)
				HOMO → LUMO+4 (52 %)
18	4.25	292	0.010	HOMO → LUMO+2 (14 %)
				HOMO → LUMO+3 (17 %)
				HOMO → LUMO+5 (56 %)
20	4.48	276	0.023	HOMO-1 → LUMO+3 (40 %)
				HOMO-1 → LUMO+5 (38 %)
21	4.56	272	0.033	HOMO-6 → LUMO (81 %)
22	4.58	271	0.011	HOMO-1 → LUMO+3 (46 %)
				HOMO-1 → LUMO+5 (34 %)
26	4.93	251	0.194	HOMO-6 → LUMO+1 (71 %)
28	5.04	246	0.014	HOMO-3 → LUMO+2 (32 %)
				HOMO → LUMO+7 (32 %)
30	5.09	244	0.016	HOMO-3 → LUMO+2 (16 %)
				HOMO → LUMO+6 (24 %)
				HOMO → LUMO+7 (17 %)
				II
2	2.04	609	0.024	HOMO-1 → LUMO (97 %)
8	3.19	388	0.100	HOMO-4 → LUMO (86 %)
9	3.40	364	0.032	HOMO-3 → LUMO+1 (92 %)
10	3.50	354	0.015	HOMO-4 → LUMO+1 (95 %)
12	3.94	314	0.014	HOMO → LUMO+2 (74 %)
15	4.14	300	0.016	HOMO-1 → LUMO+2 (12 %)
				HOMO → LUMO+4 (59 %)
18	4.31	287	0.040	HOMO-7 → LUMO (11 %)
				HOMO-6 → LUMO (82 %)
20	4.46	278	0.011	HOMO-1 → LUMO+3 (27 %)
				HOMO-1 → LUMO+5 (13 %)
				HOMO → LUMO+3 (36 %)
				HOMO → LUMO+5 (14 %)
21	4.46	278	0.014	HOMO-1 → LUMO+3 (28 %)
				HOMO-1 → LUMO+5 (13 %)
				HOMO → LUMO+3 (32 %)
				HOMO → LUMO+4 (12 %)
24	4.77	260	0.234	HOMO-6 → LUMO+1 (77 %)
25	4.83	256	0.077	HOMO-2 → LUMO+4 (52 %)
29	5.01	248	0.019	HOMO-8 → LUMO (38 %)
				HOMO-3 → LUMO+2 (38 %)
				III
3	2.13	582	0.019	HOMO-1 → LUMO (94 %)
4	2.20	563	0.012	HOMO-1 → LUMO+1 (99 %)

9	3.18	390	0.034	HOMO-4 → LUMO (93 %)
10	3.29	377	0.067	HOMO-4 → LUMO+1 (94 %)
12	3.72	334	0.019	HOMO → LUMO+2 (86 %)
20	4.35	285	0.111	HOMO-6 → LUMO (45 %)
				HOMO-6 → LUMO+1 (42 %)
22	4.47	278	0.274	HOMO-6 → LUMO (40 %)
				HOMO-6 → LUMO+1 (48 %)
23	4.49	276	0.029	HOMO-1 → LUMO+3 (13 %)
				HOMO-1 → LUMO+5 (49 %)
				HOMO → LUMO+3 (11 %)
27	4.72	263	0.037	HOMO-9 → LUMO (26 %)
				HOMO-3 → LUMO+2 (57 %)
30	4.87	254	0.023	HOMO-9 → LUMO (11 %)
				HOMO-4 → LUMO+2 (66 %)
			IV	
2	2.18	568	0.024	HOMO-1 → LUMO (98 %)
8	3.30	376	0.094	HOMO-4 → LUMO (80 %)
				HOMO-3 → LUMO (11 %)
9	3.49	355	0.026	HOMO-4 → LUMO (85 %)
10	3.54	350	0.033	HOMO-4 → LUMO+1 (84 %)
12	3.82	324	0.016	HOMO → LUMO+2 (85 %)
13	3.90	318	0.011	HOMO-1 → LUMO+2 (79 %)
14	3.91	317	0.037	HOMO-6 → LUMO (64 %)
				HOMO-5 → LUMO (11 %)
				HOMO-1 → LUMO+2 (10 %)
17	4.08	304	0.018	HOMO-6 → LUMO+1 (17 %)
				HOMO-5 → LUMO+1 (46 %)
				HOMO-1 → LUMO+3 (27 %)
18	4.10	302	0.011	HOMO-5 → LUMO+1 (14 %)
				HOMO-1 → LUMO+3 (38 %)
				HOMO → LUMO+3 (25 %)
20	4.28	290	0.580	HOMO-6 → LUMO+1 (73 %)
				HOMO-5 → LUMO+1 (17 %)
21	4.40	282	0.017	HOMO-7 → LUMO+1 (96 %)
23	4.46	278	0.025	HOMO-11 → LUMO (26 %)
				HOMO-1 → LUMO+3 (20 %)
				HOMO-1 → LUMO+4 (30 %)
27	4.80	258	0.011	HOMO-2 → LUMO+3 (56 %)
28	4.83	257	0.015	HOMO-10 → LUMO (77 %)
30	4.91	252	0.025	HOMO-3 → LUMO+2 (58 %)
				HOMO → LUMO+5 (11 %)
			V	
2	2.25	550	0.025	HOMO-1 → LUMO (98 %)
7	3.29	377	0.011	HOMO-4 → LUMO (10 %)
				HOMO-2 → LUMO+1 (82 %)
8	3.31	375	0.064	HOMO-4 → LUMO (47 %)
				HOMO-3 → LUMO (30 %)
				HOMO-2 → LUMO+1 (16 %)
9	3.57	347	0.036	HOMO-3 → LUMO+1 (82 %)
10	3.59	345	0.025	HOMO-5 → LUMO (17 %)
				HOMO-4 → LUMO+1 (76 %)
11	3.77	329	0.101	HOMO-5 → LUMO (73 %)
				HOMO-4 → LUMO+1 (11 %)
12	3.83	323	0.014	HOMO-6 → LUMO (91 %)
13	3.91	317	0.016	HOMO → LUMO+2 (81 %)

14	3.97	312	0.029	HOMO-7 → LUMO (47 %)
				HOMO-5 → LUMO+1 (16 %)
				HOMO-1 → LUMO+2 (29 %)
16	4.09	303	0.018	HOMO-1 → LUMO+2 (12 %)
				HOMO-1 → LUMO+3 (26 %)
				HOMO → LUMO+3 (37 %)
17	4.13	300	0.046	HOMO-1 → LUMO+3 (38 %)
				HOMO-1 → LUMO+4 (18 %)
				HOMO → LUMO+3 (17 %)
18	4.15	299	0.389	HOMO-7 → LUMO (13 %)
				HOMO-5 → LUMO+1 (56 %)
19	4.20	295	0.083	HOMO-6 → LUMO+1 (27 %)
				HOMO → LUMO+4 (12 %)
				HOMO → LUMO+5 (37 %)
20	4.21	295	0.070	HOMO-6 → LUMO+1 (58 %)
				HOMO → LUMO+5 (16 %)
21	4.42	280	0.013	HOMO-7 → LUMO+1 (97 %)
23	4.48	277	0.029	HOMO-1 → LUMO+3 (11 %)
				HOMO-1 → LUMO+4 (15 %)
				HOMO-1 → LUMO+5 (42 %)
25	4.62	268	0.021	HOMO-8 → LUMO (62 %)
				HOMO → LUMO+4 (20 %)
26	4.63	268	0.025	HOMO-8 → LUMO (32 %)
				HOMO → LUMO+4 (39 %)
				HOMO → LUMO+5 (18 %)
28	4.82	257	0.020	HOMO-2 → LUMO+3 (49 %)
				HOMO-2 → LUMO+4 (11 %)
30	4.94	251	0.021	HOMO-3 → LUMO+2 (66 %)

Table S4. Summary of photophysical properties for compounds **I**-**V** in different solution of DMF, MeCN, EtOH and Bz at room temperature.

Solvent	Compound	λ_{abs}/nm (ε/10^3 M^{-1} cm^{-1})	λ_{em}	$\Phi_{em, air}$	$\Phi_{em, Ar}$	τ_{air}/ns	τ_{Ar}/ns	Φ_{Δ}
DMF	**I**	361 (5.7)	566	0.041	0.264	160.6	788.3	0.66
	II	378 (4.5)	625	0.004	0.007	42.7	52.3	0.23
	III	360 (4.9)	566	0.049	0.260	178.0	991.2	0.57
	IV	369 (2.7)	612	0.012	0.023	82.1	136.1	0.39
	V	369 (3.5)	608	0.020	0.038	103.9	222.5	0.47
MeCN	**I**	366 (2.3)	582	0.013	0.068	69.1	80.5 (47%) 185.5 (53%)	0.16
	II	385 (3.6)	637	0.003	0.005	32.6	47.7	0.11
	III	379 (3.5)	582	0.005	0.021	30.7	549.4 (91%) 30.5 (8%)	0.08
	IV	377 (1.6)	618	0.011	0.044	51.6	109.8	0.21
	V	374 (5.0)	608	0.007	0.014	61.0	165.9	0.20
EtOH	**I**	371 (5.9)	593	0.013	0.026	74.1	74.3	0.20
	II	390 (5.6)	634	0.001	0.001	14.4	16.6	0.26
	III	378 (3.2)	593	0.014	0.016	71.9	69.6	0.12
	IV	382 (1.4)	550	0.028	0.008	42.2	65.9	0.62
	V	375 (3.9)	606	0.008	0.014	53.5	95.8	0.84

Bz	**I**	401 (1.0)	597	0.045	0.112	95.3	412	0.37
	II	426 (2.6)	631	0.012	0.020	65.3	123.6	0.31
	III	388 (0.5)	558	0.119	0.152	107.1	227.5	0.19
	IV	414 (1.1)	549	0.536	0.150	105.0	337.5	0.58
	V	404 (3.3)	606	0.040	0.190	113.5	529.4	0.42

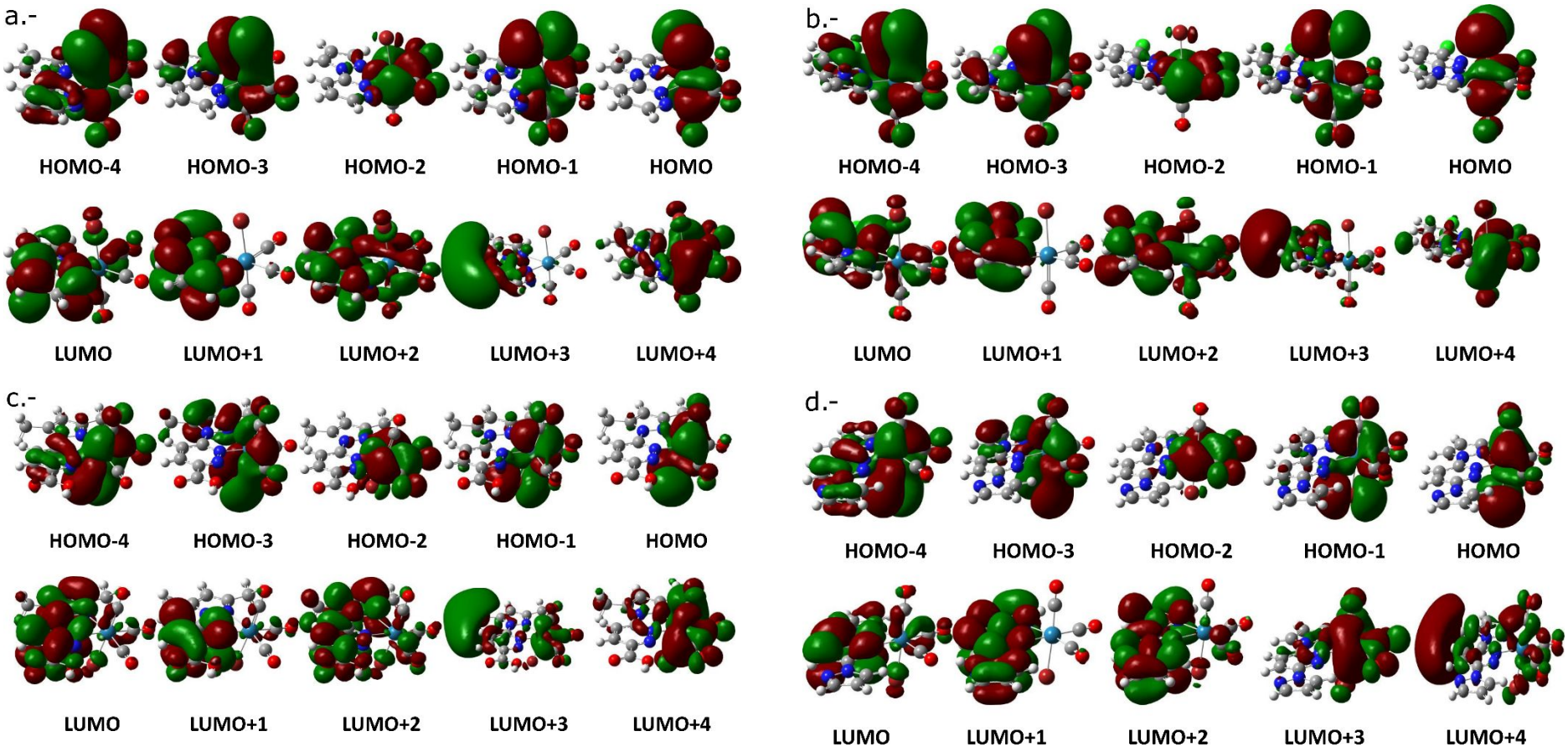
a.-
HOMO-4
HOMO-3
HOMO-2
HOMO-1
HOMO
LUMO
LUMO+1
LUMO+2
LUMO+3
LUMO+4
b.-
HOMO-4
HOMO-3
HOMO-2
HOMO-1
HOMO
LUMO
LUMO+1
LUMO+2
LUMO+3
LUMO+4
c.-
HOMO-4
HOMO-3
HOMO-2
HOMO-1
HOMO
LUMO
LUMO+1
LUMO+2
LUMO+3
LUMO+4
d.-
HOMO-4
HOMO-3
HOMO-2
HOMO-1
HOMO
LUMO
LUMO+1
LUMO+2
LUMO+3
LUMO+4

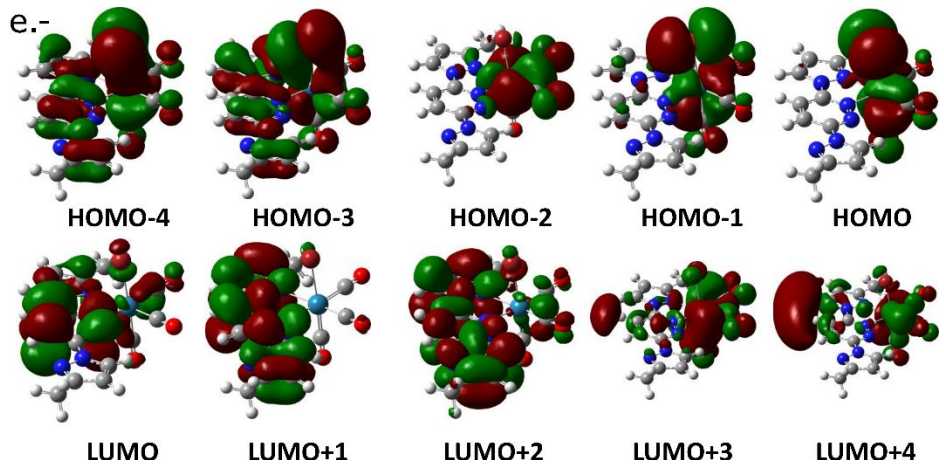

Figure S1. Frontier and near frontier Kohn-Sham orbitals for a.- **I**, b.- **II**, c.- **III**, d.- **IV** and e.- **V**.

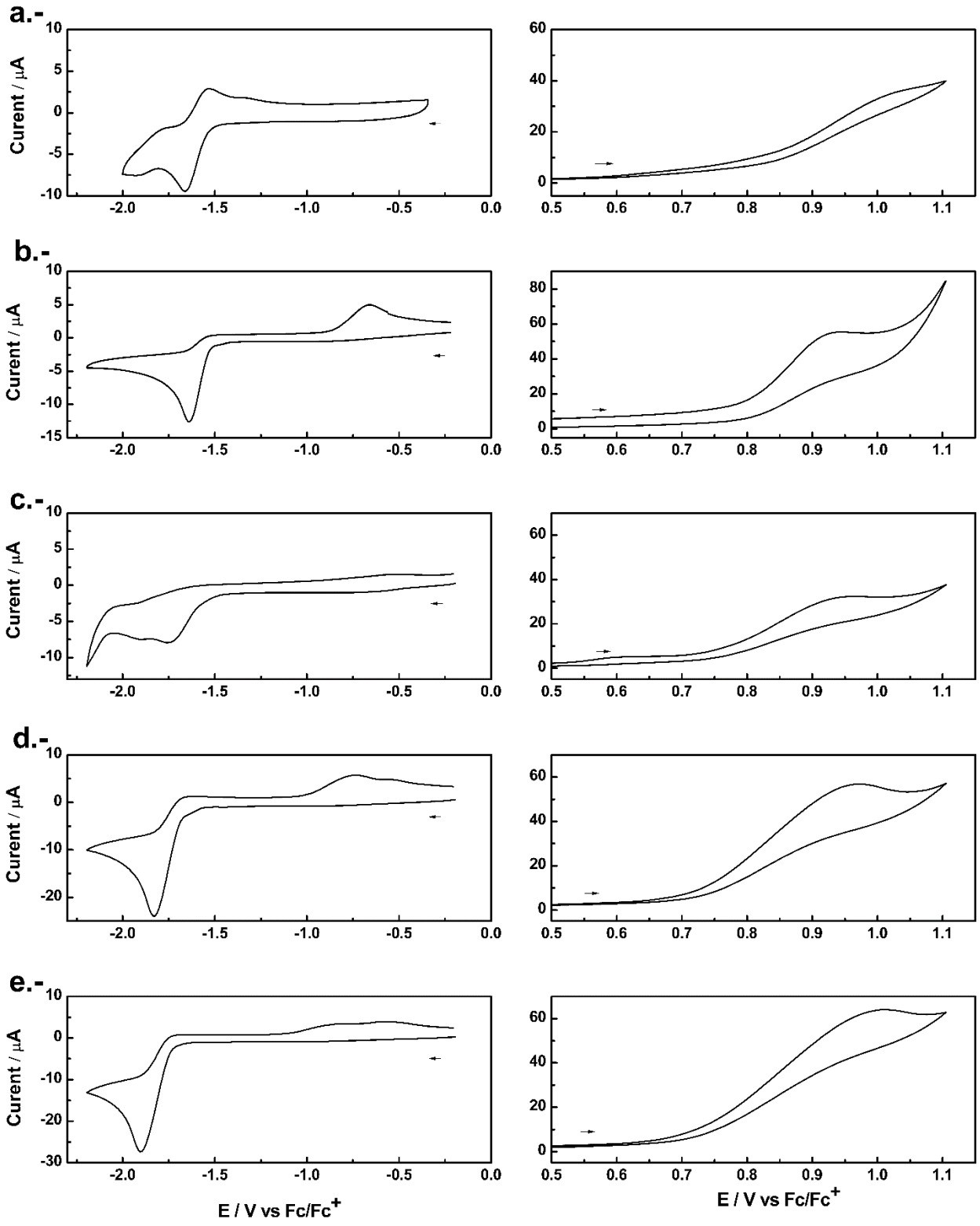

Figure S2. Cyclic voltammograms for compounds **I** (**a.-**), **II** (**b.-**), **III** (**c.-**), **IV** (**d.-**) and **V** (**e.-**), measured in N_2 saturated electrolyte solution. **Left:** cathodic scan. **Right:** anodic scan.

a.-

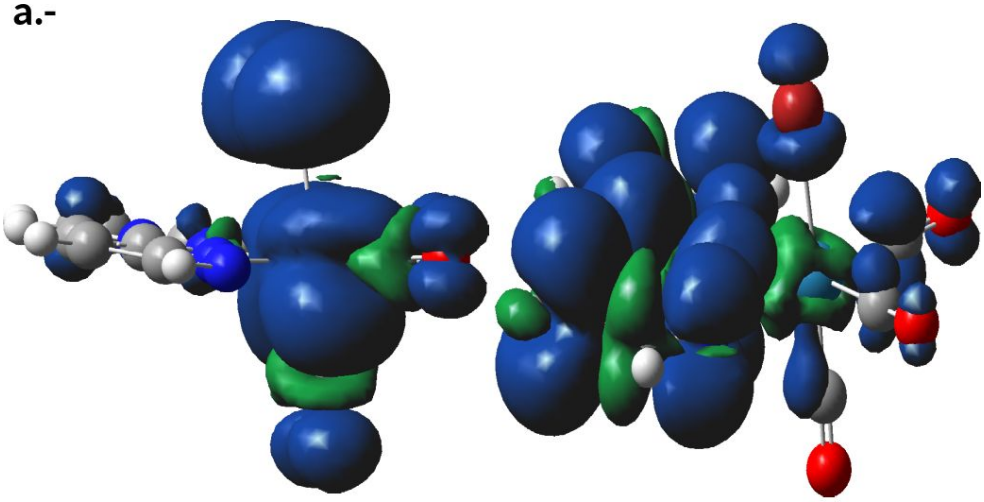

$[(L_I)Re(CO)_3Br]^{\cdot+}$ $[(L_I)Re(CO)_3Br]^{\cdot-}$

b.-

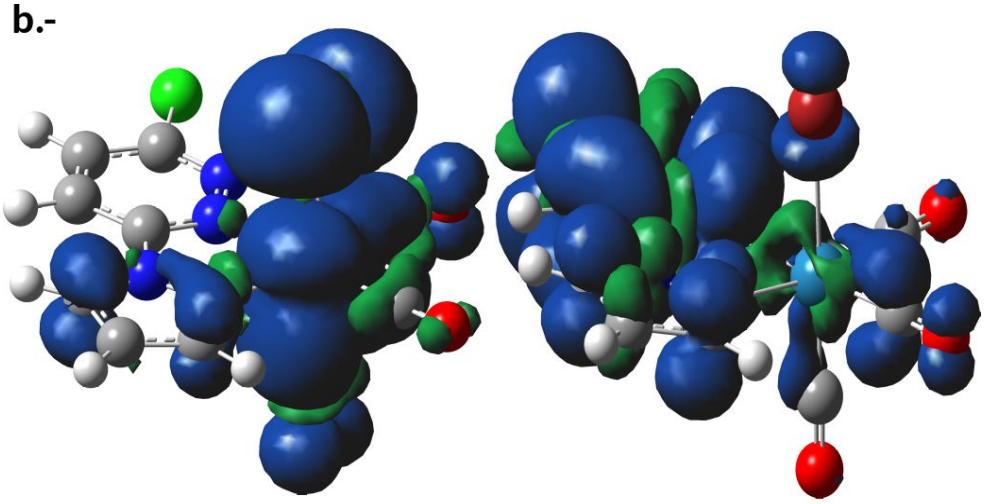

$[(L_{II})Re(CO)_3Br]^{\cdot+}$ $[(L_{II})Re(CO)_3Br]^{\cdot-}$

c.-

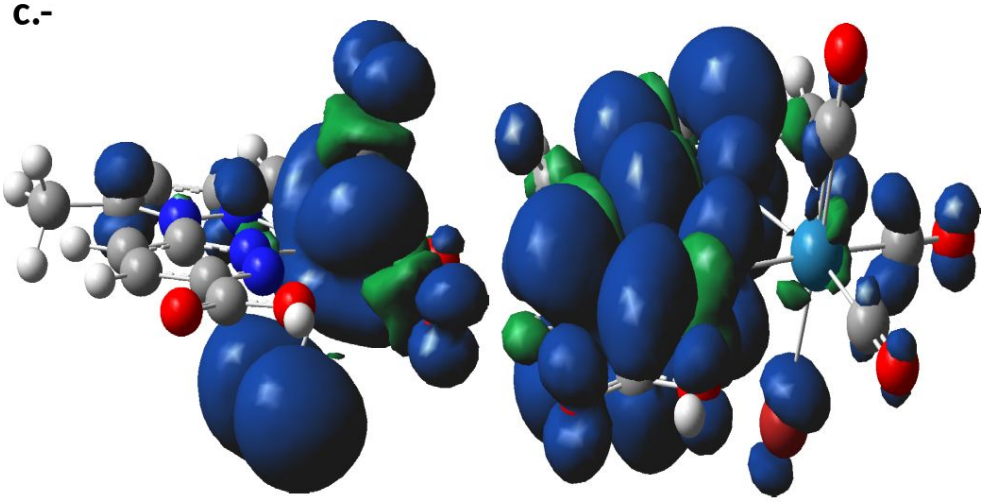

$[(L_{III})Re(CO)_3Br]^{\cdot+}$ $[(L_{III})Re(CO)_3Br]^{\cdot-}$

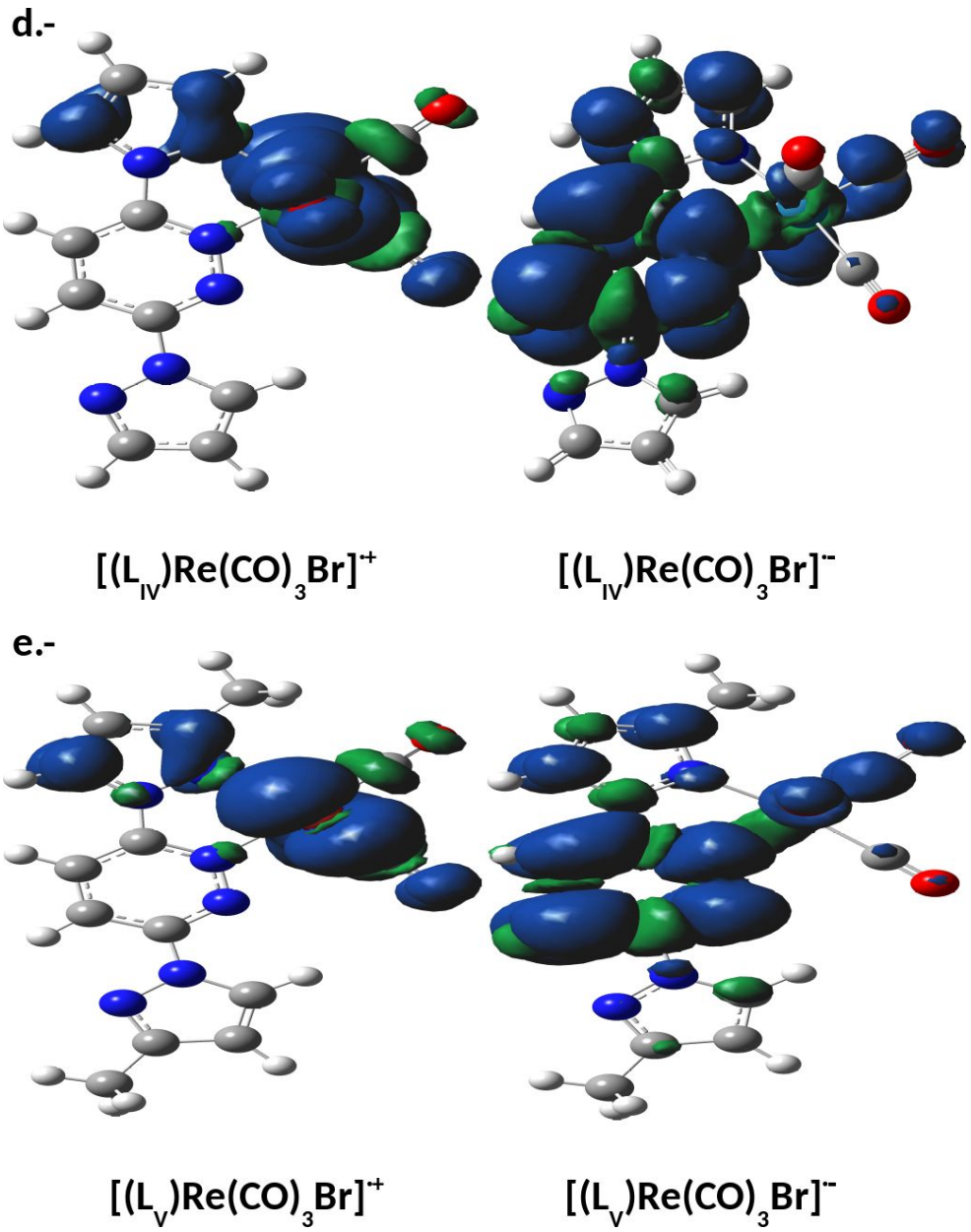

Figure S3. Gas phase DFT computed spin density transitions for the vertical reduction and oxidation a.- **I**, b.- **II**, c.- **III**, d.- **IV** and e.- **V**.

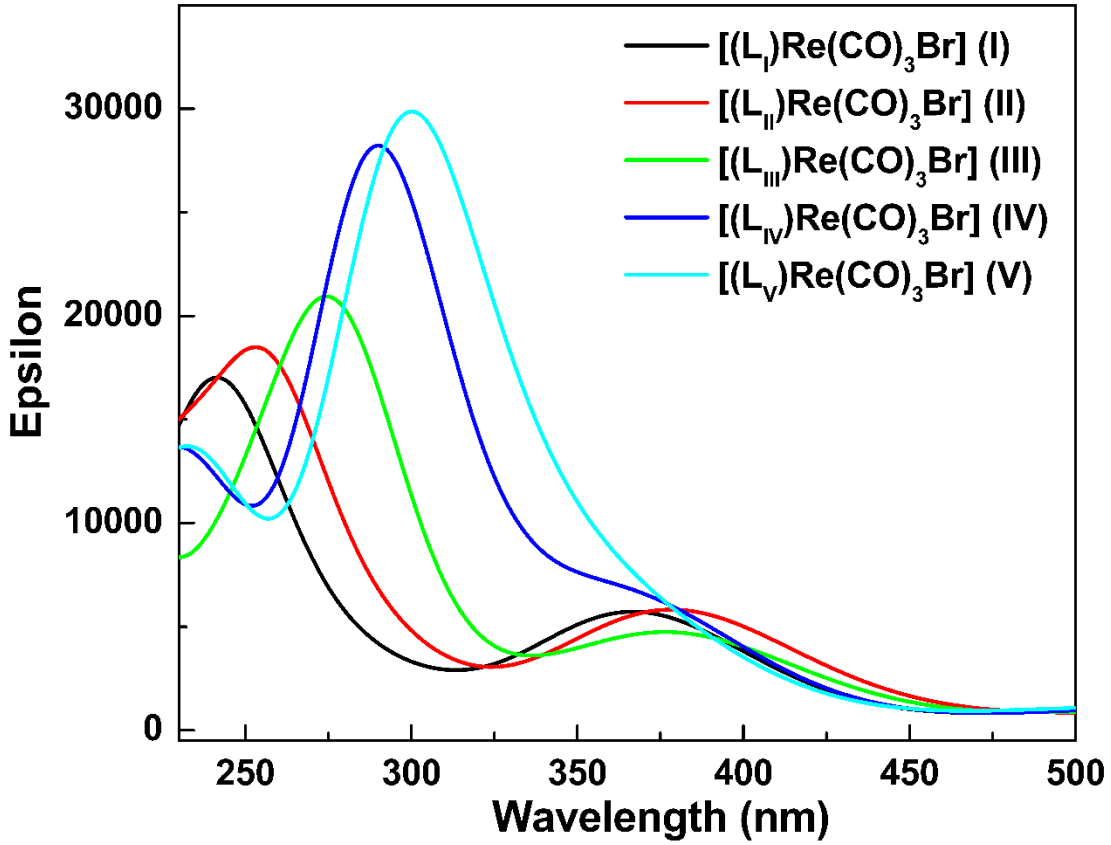

Figure S4. TD- DFT computed spectra for **I – V**.

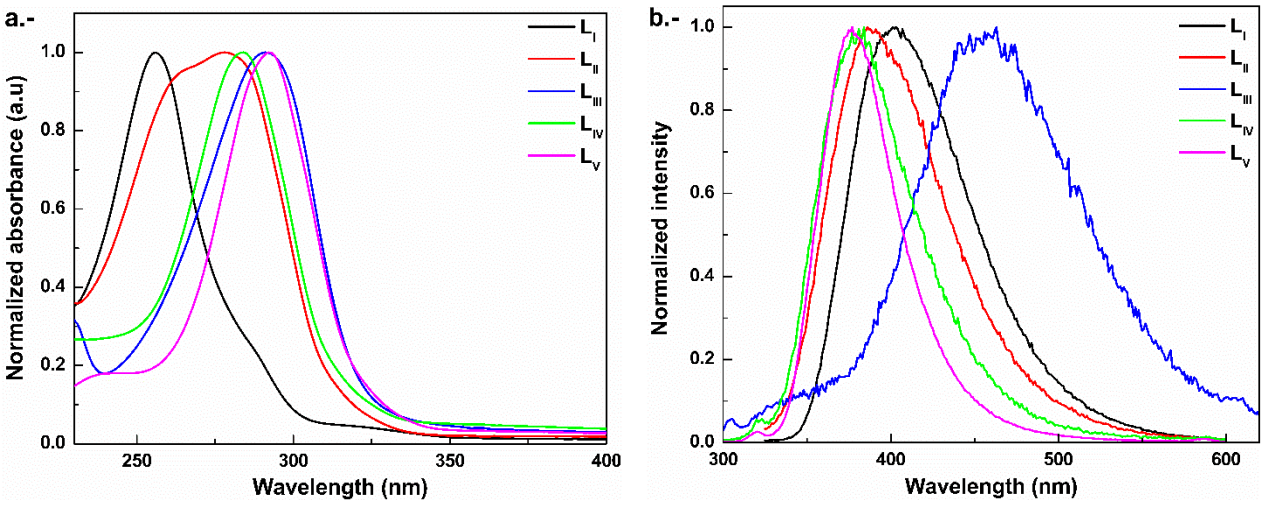

Figure S5. **a.-** Absorption and **b.-** Emission spectra for (—)**L$_I$**, (—)**L$_{II}$**, (—)**L$_{III}$**, (—)**L$_{IV}$** and (—)**L$_V$** in DCM solution after excitation at 280 nm.

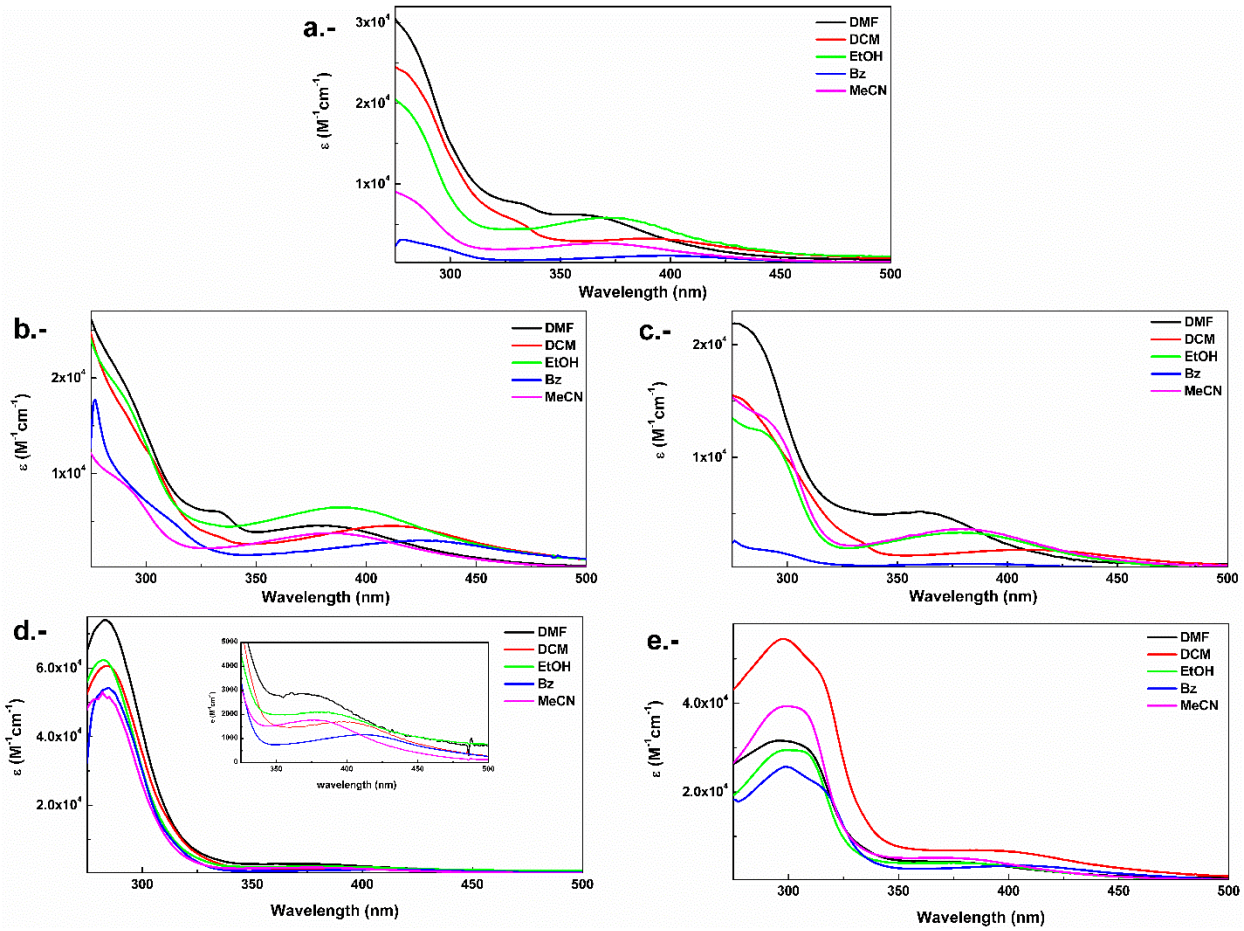

Figure S6. Absorption spectra of compounds **a.- I, b.- II, c.- III, d.- IV** and **e.- V** in air equilibrated solution in (—) DMF, (—) DCM, (—) EtOH, (—) Bz and (—) MeCN.

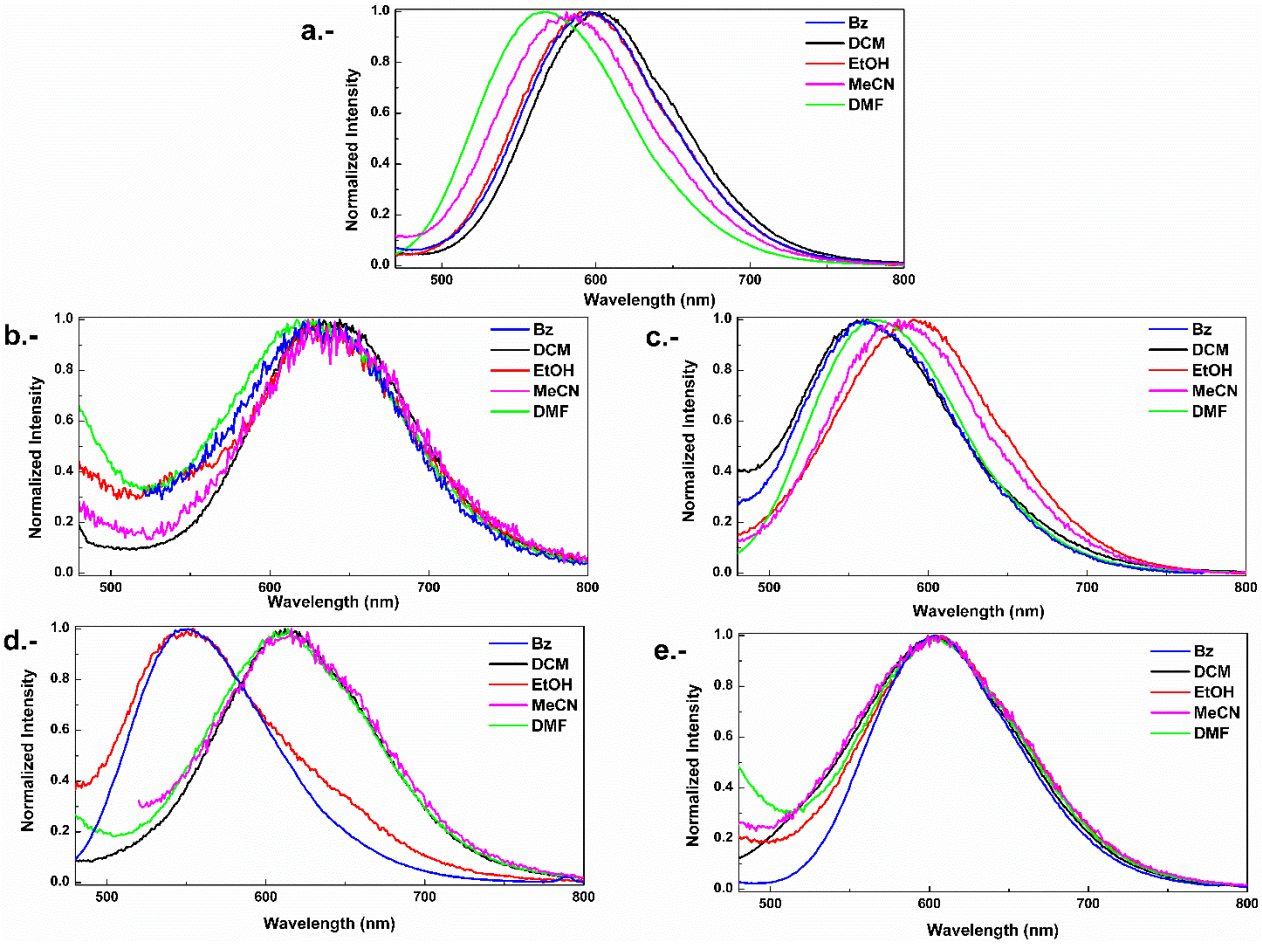

Figure S7. Emission spectra of compounds **a.- I, b.- II, c.- III, d.- IV** and **e.- V** in air equilibrated solution in (—) DMF, (—) DCM, (—) EtOH, (—) Bz and (—) MeCN. λ_{ex} = 400 nm.

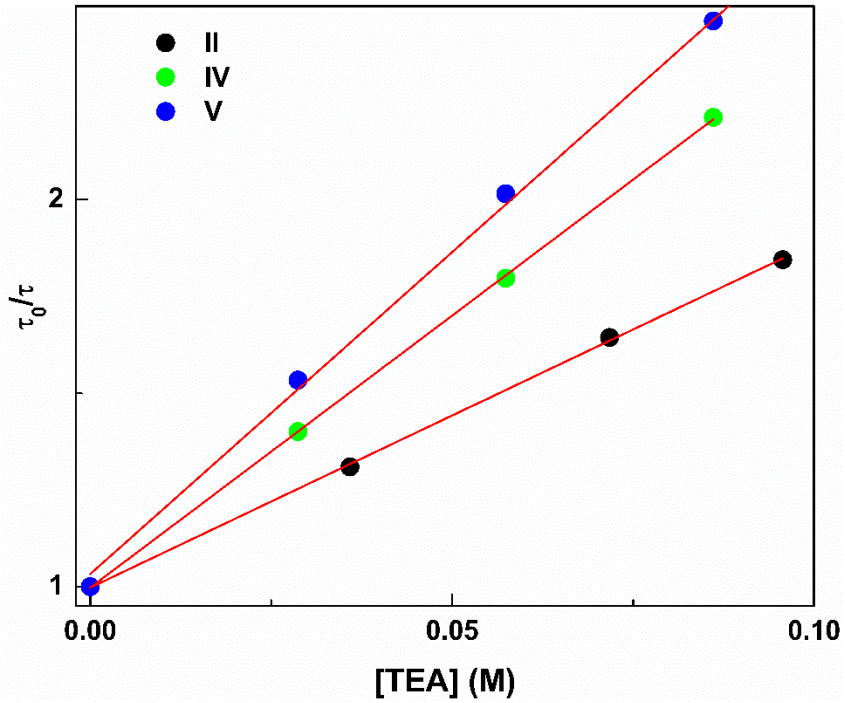

Figure S8. Stern-Volmer analysis of the TEA effect on the emission lifetimes for compounds **II, IV** and **V** in DCM solutions (λ_{exc} = 400 nm).

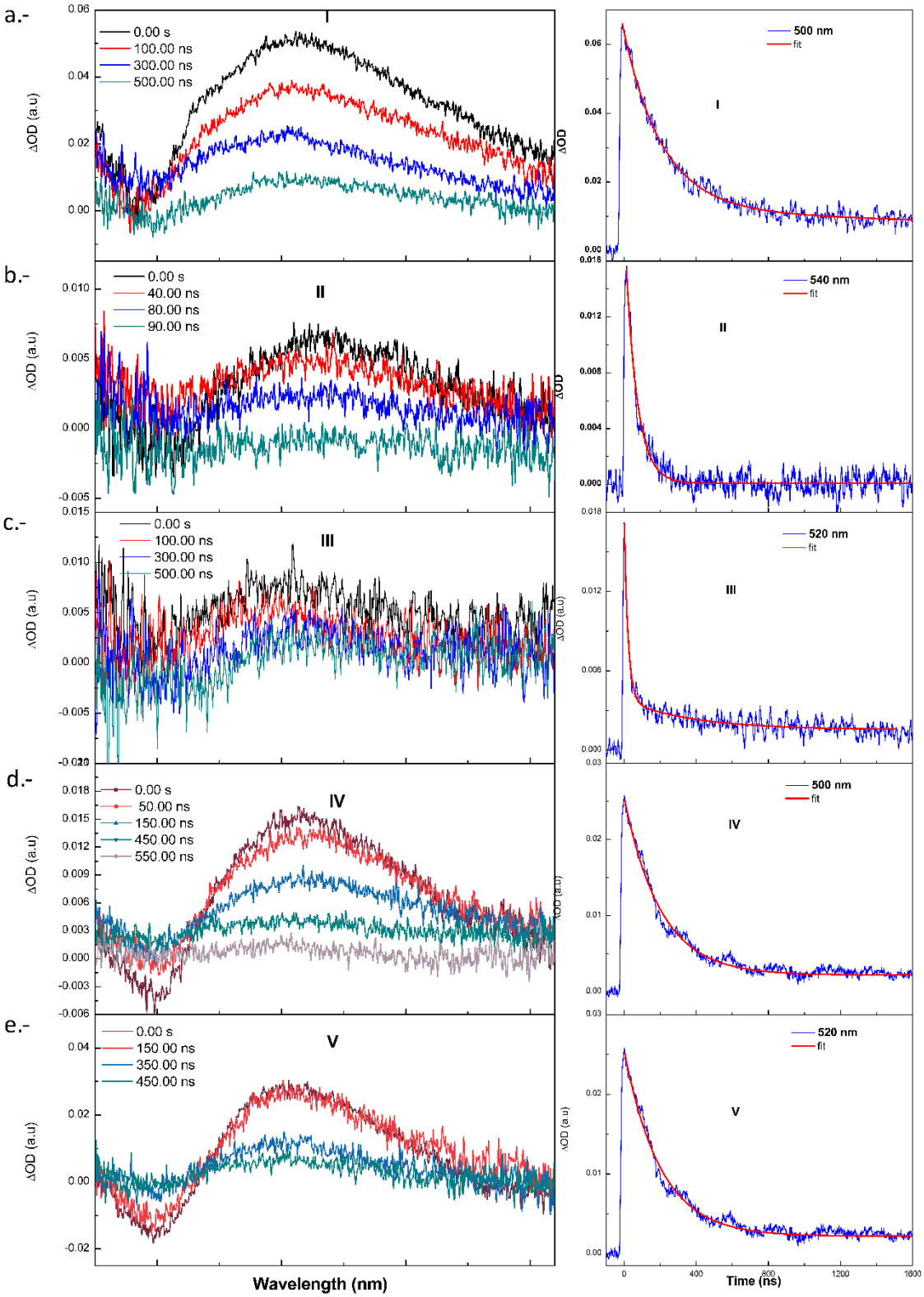

Figure S9. Transient absorption spectra (left) and traces (right) for compounds **a.- I, b.- II, c.- III, d.- IV** and **e.- V** in argon-saturated DCM solutions (λ_{exc} = 355 nm).

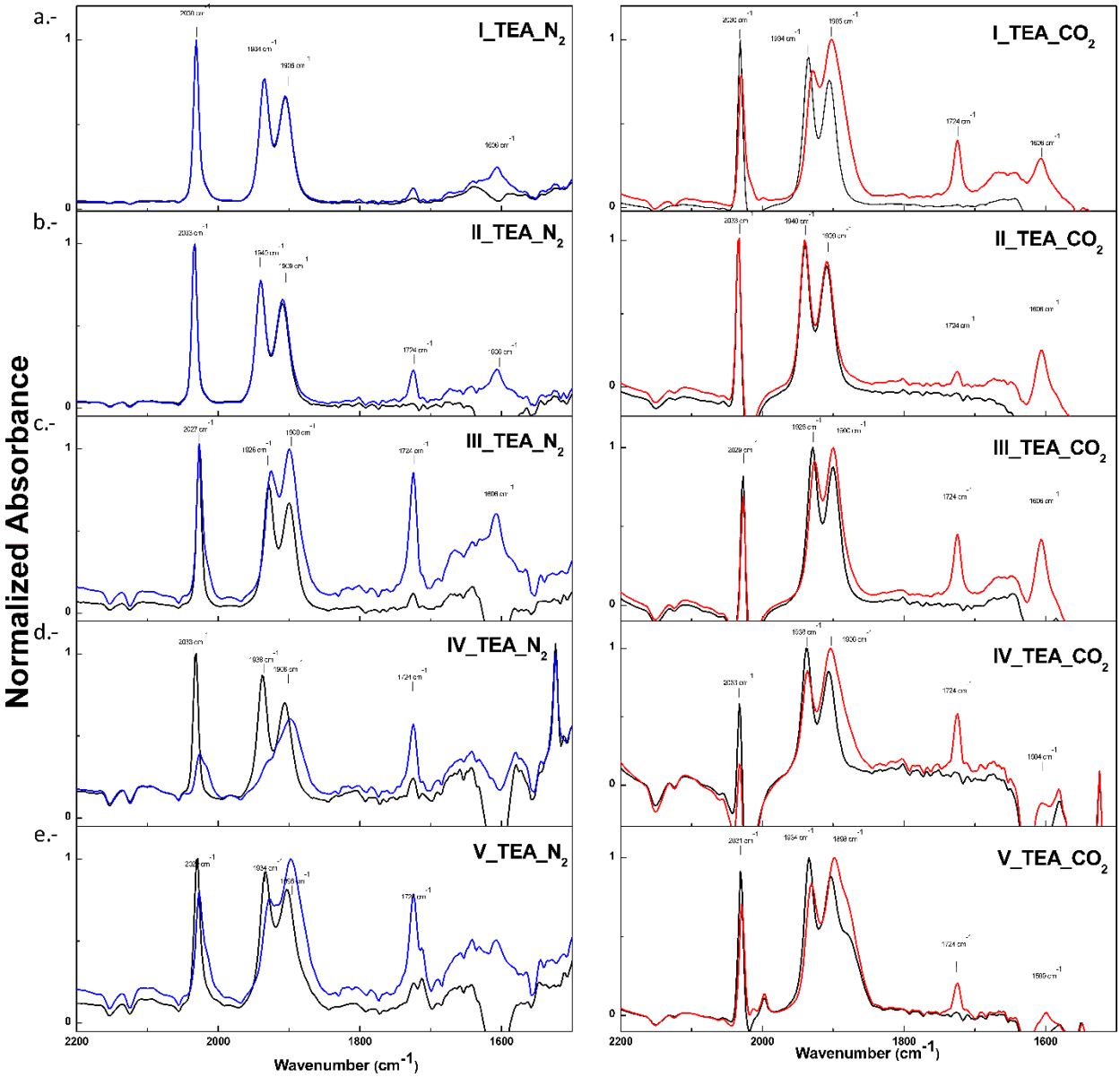

Figure S10. Photolysis experiments followed by IR for compounds **a.- I, b.- II, c.- III, d.- IV** and **e.- V** in N_2-saturated (left) and CO_2-saturated (right) DCM solutions (λ_{exc} = 350 nm for 1 hr).